3-Hydroxykynurenine and 3-Hydroxyanthranilic Acid Generate Hydrogen Peroxide and Promote α-Crystallin Cross-Linking by Metal Ion Reduction†

Lee E. Goldstein,‡,§,|| Michael C. Leopold,⊥ Xudong Huang,‡,§ Craig S. Atwood,‡,§ Aleister J. Saunders,‡,§ Mariana Hartshorn,‡,§ James T. Lim,‡,§ Kyle Y. Faget,‡,§ Julien A. Muffat,‡,§ Richard C. Scarpa,‡,§ Leo T. Chylack, Jr.,|| Edmond F. Bowden,⊥ Rudolph E. Tanzi,§ and Ashley I. Bush*,‡,§

Laboratory for Oxidation Biology, Department of Psychiatry, and Genetics and Aging Unit, Department of Neurology, Massachusetts General Hospital, Charlestown, Massachusetts 02129, Center for Ophthalmic Research, Brigham and Women's Hospital, Boston, Massachusetts 02115, and Department of Chemistry, North Carolina State University, Raleigh, North Carolina 27695

Received December 30, 1999; Revised Manuscript Received April 11, 2000

ABSTRACT: The kynurenine pathway catabolite 3-hydroxykynurenine (3HK) and redox-active metals such as copper and iron are implicated in cataractogenesis. Here we investigate the reaction of kynurenine pathway catabolites with copper and iron, as well as interactions with the major lenticular structural proteins, the α-crystallins. The *o*-aminophenol kynurenine catabolites 3HK and 3-hydroxyanthranilic acid (3HAA) reduced Cu(II)>Fe(III) to Cu(I) and Fe(II), respectively, whereas quinolinic acid and the nonphenolic kynurenine catabolites kynurenine and anthranilic acid did not reduce either metal. Both 3HK and 3HAA generated superoxide and hydrogen peroxide in a copper-dependent manner. In addition, 3HK and 3HAA fostered copper-dependent α-crystallin cross-linking. 3HK- or 3HAA-modifed α-crystallin showed enhanced redox activity in comparison to unmodified α-crystallin or ascorbate-modified α-crystallin. These data support the possibility that 3HK and 3HAA may be cofactors in the oxidative damage of proteins, such as α-crystallin, through interactions with redox-active metals and especially copper. These findings may have relevance for understanding cataractogenesis and other degenerative conditions in which the kynurenine pathway is activated.

The catabolism of tryptophan proceeds through the kynurenine pathway (Figure 1), which produces a number of toxic metabolic intermediates including 3-hydroykynurenine (3HK),[1] 3-hydroxyanthranilic acid (3HAA), and quinolinic acid (QA) (*1*). A diverse set of findings implicates the kynurenine pathway and tryptophan catabolites in a variety of neurodegenerative, inflammatory, and immunologic phenomena including Huntington's Disease (*2, 3*), Parkinson's Disease (*4*), HIV encephalopathy (*5*), cerebral malaria (*6*), poliomyelitis (*7, 8*), and fetomaternal tolerance (*9*). Animal models of multiple sclerosis (*10*) and viral pneumonia (*11*) have also demonstrated activation of the kynurenine pathway. Both 3HK and 3HAA cause neuronal cell death with apoptotic features in primary neuronal cultures (*12, 13*).

Kynurenine pathway catabolites and their *o*-*β*-glucoside derivatives are found in the ocular lens (*14*−*17*), where the kynurenine pathway is constitutively active in the anterior cortical epithelial cells (*18*). 3HK is present in primate lens in the micromolar concentration range (*17*−*19*). In the lens, 3HK and its glucoside interact with lysyl residues of the lens proteins (*20*) and may function as a shortwave ultraviolet light filter (*14, 21*) absorbing maximally at approximately 365 nm. 3HK has been shown to foster formation of protein aggregates which may contribute to the brunescent color of cataractous lens (*20*). A recent study demonstrated that the amount of 3HK glucoside bound to the lenticular proteins increases with age (*22*). Thus, speculation has arisen as to the possible relevance of 3HK in the pathogenesis of age-related cataracts (ARC).

During cataractogenesis, α-crystallin undergoes a conformational transition from a soluble protein found in the transparent lens to a colored, insoluble, highly cross-linked aggregate (*23*−*26*). α-Crystallin is composed of two subspecies, α_A (aa: 173; M_w: 19 909) and α_B (aa: 175; M_w: 20 159), in a molar ratio which is variable among species (*27*). These proteins exhibit chaperone and protein surfactant functions (*28, 29*). α_A-Crystallin is found predominantly in the ocular lens, whereas α_B-crystallin is also found in

†This work is supported by funds from the American Federation for Aging Research/Alliance for Aging Research (Paul Beeson Physician Faculty Scholar in Aging Research Award to A.I.B.), the Consolidated Departments of Psychiatry, Harvard Medical School (Dupont-Warren Award to L.E.G.), the American Health Assistance Foundation, and the PRANA Corporation.

* Correspondence should be addressed to this author at the Laboratory for Oxidation Biology, Massachusetts General Hospital-East, Building 149, 13th St., Charlestown, MA 02129. Ph: (617) 726-8244; Fax: (617) 724-9610; e-mail: bush@helix.mgh.harvard.edu.

‡ Laboratory for Oxidation Biology, Massachusetts General Hospital.

§ Genetics and Aging Unit, Massachusetts General Hospital.

|| Center for Ophthalmic Research, Brigham and Women's Hospital.

⊥ Department of Chemistry, North Carolina State University.

[1] Abbreviations: ANA, anthranilic acid; ARC, age-related cataracts; ASC, ascorbic acid; BC, bathocuproine; BCA, bicinchoninic acid; BP, bathophenanthroline; BSA, bovine serum albumin; DCF, dichlorofluorescein diacetate; DTPA, diethylenetriaminepentaacetic acid; 3HAA, 3-hydroxyanthranilic acid; 3HK, 3-hydroxykynurenine; ITO, indium/tin oxide; KYN, L-kynurenine; KA, kynurenic acid; PBS, phosphate-buffered saline; QA, quinolinic acid; ROS, reactive oxygen species; TETA, triethylenetetramine; XA, xanthurenic acid.

10.1021/bi992997s CCC: $19.00
Published on Web 05/26/2000

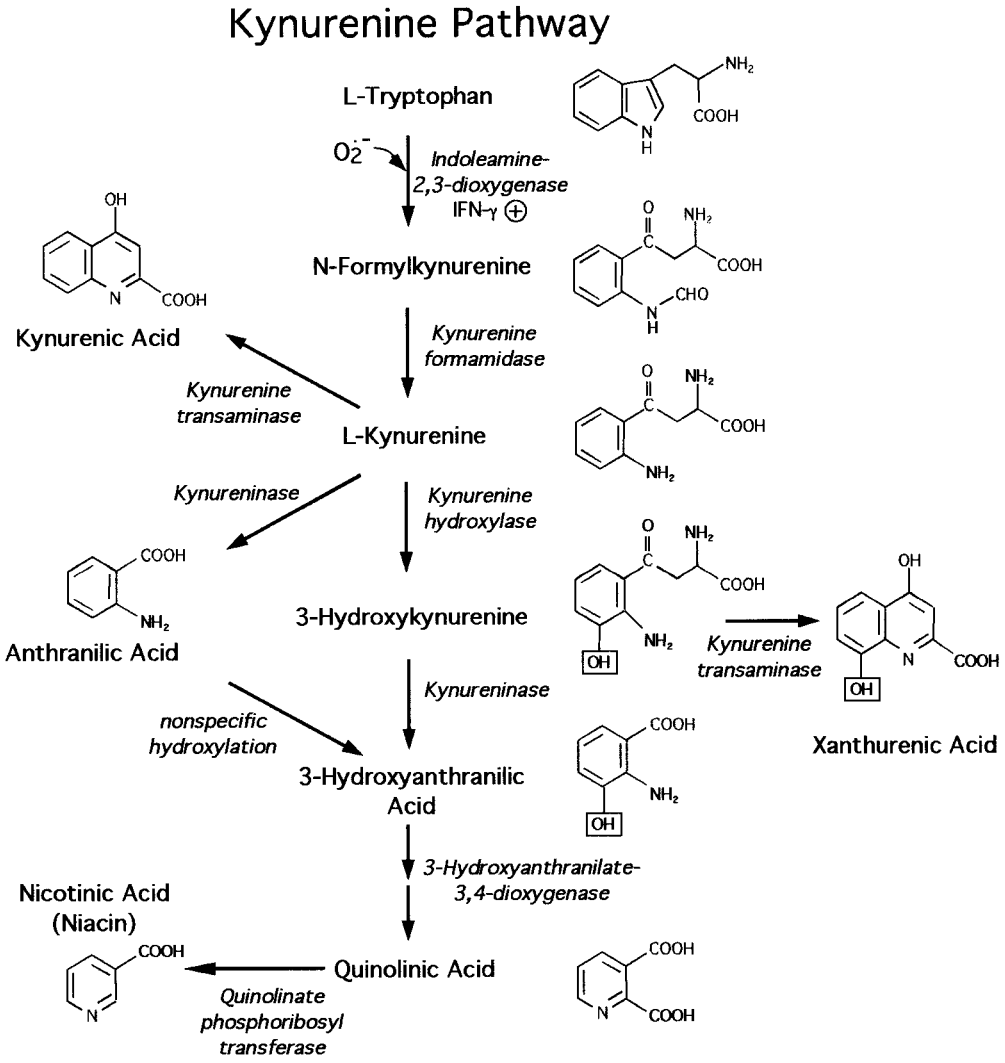

FIGURE 1: Tryptophan metabolism through the kynurenine pathway. Enzymes catalyzing reactions are indicated in italic. The rate-limiting reaction is catalyzed by indoleamine-2,3-dioxygenase, which requires the presence of superoxide and is upregulated by interferon gamma (IFN-γ). The phenolic hydroxyl group is noted by a box on the compounds that reduce Cu(II) to Cu(I) and generate hydrogen peroxide.

extralenticular tissues including heart, muscle, and brain (*30*) and shares homology with and functions as a heat-shock protein (*31*).

In addition to protein aggregation, cataract formation is also characterized by oxidative damage. Decreases in the level of antioxidant defense enzymes such as glutathione reductase, glutathione peroxidase, and superoxide dismutase, as well as decreases in total glutathione and corresponding increases in oxidized glutathione, have been observed (*32*−*34*). Evidence of oxidative damage includes increased lenticular lipid peroxidation markers such as malondialdehyde (*35*), and increased concentration of hydrogen peroxide in the aqueous humor (*34, 36, 37*). Numerous studies have also demonstrated elevated levels of total copper in cataractous lens (*38*−*45*). This finding is important as Cu(II) is a cofactor in generating potentially damaging reactive oxygen species (ROS), such as hydrogen peroxide and superoxide, which may foster protein aggregation as noted in other systems [e.g., the Alzheimer's Disease A$\beta_{(1-42)}$ protein (*46*)]. This evidence suggests that increased oxidative stress and the accumulation of copper (or other redox-active metals such as iron) in the lens may participate in ARC-related crystallin aggregation. Here we explore possible biochemical interactions between 3HK (and related kynurenine catabolites) and the redox-active transition metals Cu(II) and Fe(III), to determine whether these factors may contribute to ROS generation and aggregation of α-crystallins as observed in ARC.

Our results demonstrated that the *o*-aminophenol kynurenine metabolites 3HK and 3HAA, but not their nonphenolic precursors kynurenine (KYN) or anthranilic acid (ANA), reduced Cu(II) and Fe(III) at physiological pH, subsequently generating superoxide and hydrogen peroxide in a copper-dependent manner. Furthermore, both 3HK and 3HAA potentiated Cu(II)-dependent cross-linking of α_B-crystallin. These findings may have relevance for understanding ARC, as well as inflammatory and immunological processes in which the kynurenine pathway is activated.

EXPERIMENTAL PROCEDURES

Materials. Metal ion standard solutions (10 mg/mL in 10% HNO_3) were purchased from the National Institute of Standards and Technology, Gaithersburg, MD. The hydrogen peroxide indicator 2′,7′-dichlorofluorescein diacetate (DCF) was purchased from Molecular Probes, Eugene, OR. Total lens protein was freshly prepared from a calf eye obtained from a local abbatoir. The lens was dissected out and

homogenized in chilled PBS, pH 7.4, with added protease inhibitor cocktail with a ground glass tissue homogenizer and immediately frozen and stored at −80 °C. Recombinant human α_B-crystallin was the generous gift of Dr. J. Liang, Brigham and Women's Hospital, Boston, MA (*47*). Polyclonal rabbit antibodies directed against either α_A-crystallin or α_B-crystallin were the generous gift of Dr. J. Horwitz, University of California, Los Angeles. All other reagents were purchased from Sigma, St. Louis, MO, unless otherwise noted. All solutions were prepared in filter-sterilized, Chelex-treated (Chelex 100 resin, Bio-Rad, Hercules, CA) Dulbecco's phosphate-buffered saline without calcium or magnesium (PBS: KCl 2.7 mM, KH_2PO_4 1.4 mM, NaCl 137 mM, Na_2HPO_4 7.68 mM), pH adjusted to 7.4. Cu(II)-Gly and Fe(III)-citrate stock solutions were used to prevent metal−hydroxy and metal−oxy polymers that form in neutral metal ion solutions. Working stock solutions of Cu(II)-glycine or Fe(III)-citrate metal ions were prepared in PBS, pH 7.4, by dilution of the standard metal ion stocks with ligands in a molar ratio of 1:6.

Metal Reduction Assays. Assays were performed using a 96-well microtiter plate (Costar, MA). Test compounds from the kynurenine pathway (10 μM) or, as a positive control, ascorbic acid (ASC, 10 μM) were coincubated with either Fe(III)-citrate (25 μM) and the Fe(II) indicator bathophenanthroline disulfonic acid (BP, 250 μM), or Cu(II)-glycine (25 μM) and the Cu(I) indicator bathocuproine disulfonic acid (BC, 250 μM) or bicinchoninic acid (BCA, 250 μM). Incubations were conducted in PBS, pH 7.4 at 37 °C, in the dark for 1 h. Absorbances were then measured using a plate reader (SPECTRAmax Plus, Molecular Devices, CA) at the appropriate wavelengths: Fe(II)-BP complex at 535 nm (the known molar absorption coefficient, M_{535}, = 22 140 M^{-1} cm^{-1}), Cu(I)-BC complex at 483 nm (M_{483} = 12 250 M^{-1} cm^{-1}), or Cu(I)-BCA complex at 562 nm (M_{562} = 7700 M^{-1} cm^{-1}). In control samples, absorbances from the metal ion and indicator in the absence of test compound and the absorbance of test compound in the presence of metal ions but in the absence of indicator were determined. The absorbances from these controls were deducted from those obtained in the presence of the test compound, metal, and indicator to yield the net absorbance (ΔA). Fe(II) or Cu(I) concentrations (μM) were calculated according to the formula: $C(\mu M) = (\Delta A \times 10^6)/M_\lambda$.

Cyclic Voltammetry. Cyclic voltammetry was performed at room temperature (22 ± 2 °C) on ambient solutions using an EG&G PAR potentiostat, model 273. The potentiostat was operated in ramp mode, generating a potential staircase waveform with a 0.25 mV step height. The potential window of +0.15 to −0.4 V, in which Cu(II) is electroactive but the catabolites are not, was scanned in both directions at a rate of 100 mV/s. The current response was passed through a 5.3 Hz low-pass filter. A minimum of three cycles were collected for each scan, ensuring the stability of the electrochemical response. The electrochemical cell consisted of an indium/tin oxide (ITO) working electrode (Delta Technologies) with an active area of 0.32 cm^2, a platinum wire auxiliary electrode, and a Ag/AgCl (1 M KCl) reference electrode (Microelectrodes Inc.). Both the auxiliary and reference electrodes were positioned in the cell in close proximity to the working electrode. The working electrodes were pretreated with successive 10 min sonications in Alconox (≈8 g/L), 95% ethanol, Milli-Q-purified H_2O (2×), and PBS (pH 7.4), followed by an overnight soak in PBS (pH 7.4). The ITO electrodes were subsequently activated immediately prior to use by successive cycling in PBS in each of the following potential windows: (+0.15 to −0.4 V), (+0.4 to −0.4 V), and (+1.0 to −0.4 V). Copper(II) chloride (25 μM, Allied Chemical) was used as the Cu(II) source. Background voltammograms were obtained on each new electrode before testing the kynurenine pathway catabolites. PBS solutions of KYN, 3HK, ANA, and 3HAA (each at 100 μM) were separately scanned with and without added Cu(II). Each experiment also included a scan of Cu(II) (25 μM) in PBS without added test compound. All solutions were tested within minutes of being prepared. Each test was repeated to ensure the reproducibility of the results.

Superoxide Assay. The fluorometric assay for superoxide is based upon the dihydroethidium (DHE, Hydroethidine) method (Molecular Probes, Eugene, OR) and used according to the manufacturer's instructions. This method is specific for detection of superoxide (*48*). DHE (1 mM) was freshly prepared in 100% argon-sparged DMSO. The reaction solutions were carried out in oxygen-saturated PBS, pH 7.4, in 96-well format plates and contained a test compound (3HK, KYN, 3HAA, ANA, or XA each at 10 μM), DHE (100 μM), ± Cu(II)-glycine (1 μM), ± the copper chelator DTPA (200 μM), and catalase (100 IU/mL), and were then incubated at 37 °C for 120 min. Reactions were conducted in the dark to avoid photodynamic effects. The fluorescent readings were recorded by a Packard FluoroCount fluorescent plate reader with a 510 nm excitation filter and a 590 nm emission filter.

Hydrogen Peroxide Assay. The fluorometric assay for hydrogen peroxide is based on the dichlorofluorescein diacetate (DCF) method (Molecular Probes, Eugene, OR). The DCF solution (5 mM) in 100% ethanol was deacetylated in the presence of 0.01 M NaOH for 30 min and neutralized. Horseradish peroxidase (200 units/mL) was then added and the DCF concentration adjusted to 200 μM in PBS. The reaction solutions were carried out in in PBS, pH 7.4, in a 96-well format plate (total volume = 200 μL/well) and contained a test compound (KYN, 3HK, 3HAA, ANA, or ASC each at 10 μM), deacetylated DCF (20 μM), and Cu(II)-glycine (1 μM) and were incubated at 37 °C for 60 min. Reactions were conducted in the dark to avoid photodynamic effects. Abolition of the reading by coincubation with catalase (1000 units/mL) was used for establishing H_2O_2 specificity. The fluorescent readings were recorded by a Packard FluoroCount fluorescent plate reader with a 485 nm excitation filter and 530 nm emission filter. Concentrations were determined by comparison to a standard curve using reagent grade hydrogen peroxide in Chelex-treated PBS buffer, pH 7.4.

α-Crystallin Cross-Linking Studies. Frozen stock aliquots of recombinant human α_B-crystallin or freshly prepared bovine (calf) total lens protein were dissolved to final concentrations of 25 μg/mL (for the experiments involving recombinant α_B-crystallin) or 100 μg/mL (for the experiments with total lens protein). Various solutions containing 3HK (10 μM) or other kynurenine pathway catabolites (10 μM), Cu(II)-glycine (10 μM), Fe(III)-citrate (10 μM), and triethylenetetramine (TETA, 200 μM), were added in combinations as indicated. All solutions were prepared under sterile

conditions in a laminar flow tissue culture hood in a final volume of 1.0 mL of sterile PBS and placed in sterile 1.5 mL translucent siliconized Eppendorf tubes. Solutions were incubated in a humidified incubator for 5 days at 37 °C in the dark to avoid photodynamic effects. After incubation, aliquots of the total lens protein solutions were mixed with sample buffer containing 4% SDS and 5% β-mercaptoethanol, heated to 95 °C for 5 min, and loaded at 1 μg/lane on a 10−20% Tricine gel (Novex, San Diego, CA) and electrophoresed according to manufacturer's recommendations. The gels were then electroblotted to poly(vinylidene difluoride) membranes using a Bio-Rad transblot cell, fixed, blocked with 10% milk, and then probed with a 1:1000 dilution of polyclonal rabbit anti-α_B-crystallin antibody overnight at 4 °C. The blot was then washed and incubated with anti-rabbit horseradish peroxidase conjugate (Pierce, Rockford, IL) for 2 h at room temperature. Chemiluminescent detection was carried out using SuperSignal Ultra (Pierce) according to the manufacturer's instructions. For the experiments with recombinant α_B-crystallin, aliquots of the protein solutions were mixed with NuPAGE sample buffer (Novex, San Diego, CA) with 10% β-mercaptoethanol, heated to 95 °C for 5 min, spun briefly, then loaded on a NuPAGE 4−12% Bis-Tris polyacrylamide gel at 375 ng/lane, and electrophoresed with denaturing 3-(*N*-morpholino)propanesulfonic acid (MOPS)−SDS running buffer according to the manufacturer's recommendations. Gels were stained for total protein using Bio-Rad Silver Stain Plus (Hercules, CA) according to the manufacturer's recommendation.

Studies of Tanned Calf Lens Crystallin. α-Crystallin (10 mg/mL) from calf lens was modified by reaction with 3HK (100 μM), 3HAA (100 μM), or ASC (100 μM) in PBS, pH 7.4, for 12 h at 4 °C in the dark. Control samples were incubated with ascorbic acid (100 μM) or without added reductant. The tanning incubation solutions also contained the copper chelator triethylenetetraamine (TETA, 200 μM) to prevent cross-linking of the protein. After incubation, free reductant was removed from the tanned α-crystallin preparations by exhaustive dialysis at 4 °C in the dark utilizing PBS, pH 7.4, containing Chelex 100 chelating ion-exchange resin (Bio-Rad). The various modified α-crystallin preparations (100 μg/mL) were then assayed for metal reduction capacity using the BC and BP spectrophotometric assay as detailed above. Incubated and dialyzed α-crystallin (100 μg/mL) and untreated α-crystallin (100 μg/mL) preparations were used for procedural control.

RESULTS

The compounds comprising the kynurenine pathway (Figure 1) were assayed for their ability to reduce Fe(III) and Cu(II) (Figure 2A). The *o*-aminophenol kynurenine catabolites, 3HK and 3HAA, potently reduced Cu(II) (100%) and Fe(III) (approximately 50%), whereas the dihydroxyquinaldic acid kynurenine catabolite, xanthurenic acid (XA), reduced Cu(II) approximately 40% but did not reduce Fe(III). The high-affinity cationic metal chelator diethylenetriaminepentaacetic acid (DTPA) and the high-affinity Cu(II) chelator triethylenetetramine (TETA) both abolished metal reduction by 3HK, 3HAA, and XA (Figure 2B), indicating that the signal observed was due to metal reduction and not to a nonspecific interaction of the active metabolites with the indicator compounds. The reduction of Fe(III) and Cu(II) by ascorbic acid (ASC), the positive control, was also abolished by chelation. 3HK and 3HAA, each at 10 μM, were able to reduce 25 μM Cu(II), suggesting that more than one electron is transferred from these tryptophan metabolites to Cu(II). The other kynurenine catabolites were ineffective reducing agents for either Cu(II) or Fe(III). Since BC could potentially increase the oxidation potential of Cu(II) (*49*), we employed the bicinchoninic acid (BCA) assay to corroborate Cu(II) reduction and found that the reduction efficiencies of the agents examined were in close agreement with the values determined by the bathocuproine method (Figure 2A).

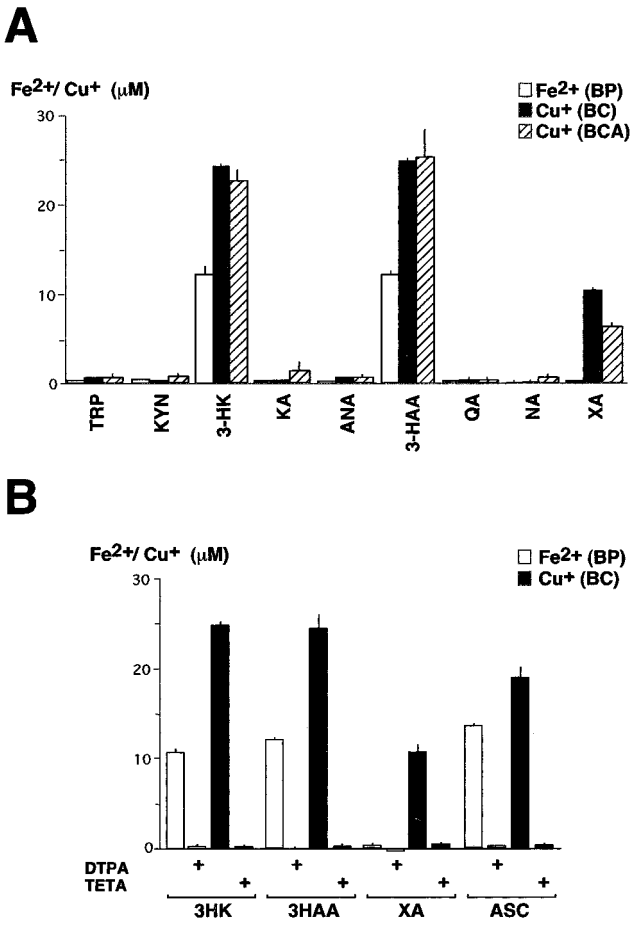

FIGURE 2: Reduction of Cu(II) and Fe(III) by kynurenine pathway catabolites. In panel A, the kynurenine pathway catabolites were tested for ability to reduce Cu(II) and Fe(III) to Cu(I) and Fe(II), respectively. Test compounds (10 μM) were coincubated with either Fe(III)-citrate (25 μM) or Cu(II)-glycine (25 μM) for 1 h in the dark at 37 °C in the presence of reduced metal indicators (BP, bathophenanthroline; BC, bathocuproine; BCA, bicinchoninic acid). Panel B shows the effect of the metal chelator diethylenetriaminepentaacetic acid (DTPA, 250 μM) and the Cu(II) chelator triethylenetetramine (TETA, 250 μM) upon the reduction of 3HK, 3HAA, XA, and ASC. Values represent the mean ± SD for three independent measurements. Abbreviations: TRP, L-tryptophan; KYN, L-kynurenine; 3HK, 3-DL-hydroxykynurenine; KA, kynurenic acid; ANA, anthranilic acid; 3HAA, 3-hydroxyanthranilic acid; QA, quinolinic acid; NA, nicotinic acid; XA, xanthurenic acid; ASC, ascorbic acid.

Our data indicated that the aminophenol kynurenine catabolites 3HK and 3HAA are the strongest Cu(II) reducing agents in the pathway. Therefore, to confirm the observed redox activities of 3HK and 3HAA, cyclic voltammetry was employed to further characterize the interaction of these catabolites with Cu(II) (Figure 3). The voltammograms in

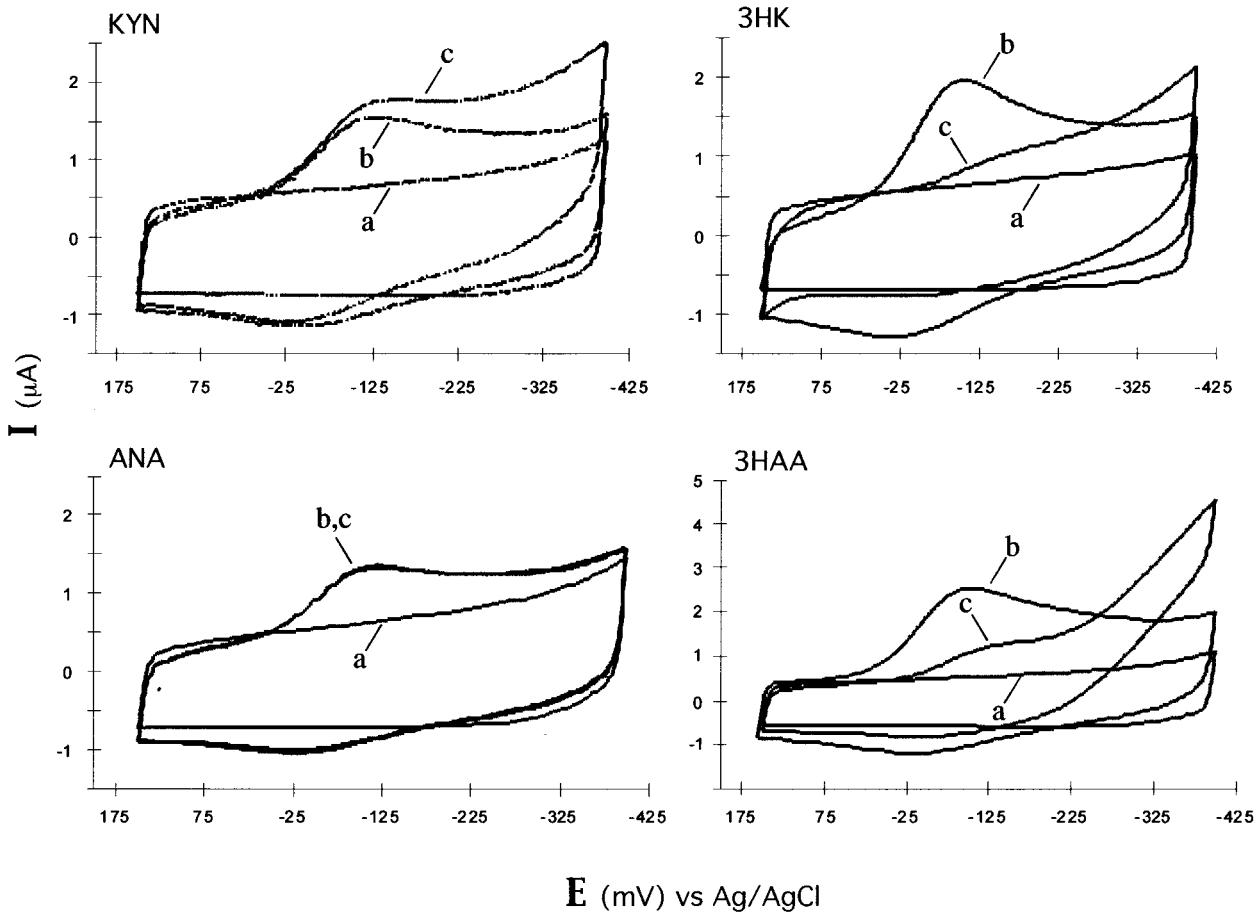

FIGURE 3: Cyclic voltammetry analysis of kynurenine pathway catabolites in the presence of Cu(II). Cyclic voltammetry was conducted at pH 7.4 with copper(II) chloride (25 μM) ± KYN, 3HK, ANA, and 3HAA (100 μM). In each panel, voltammograms are shown for (a) background current in PBS, (b) Cu(II) in PBS, and (c) Cu(II) in the presence of each of the designated catabolites. Note the different current scale for the 3HAA voltammogram.

Figure 3 compared 3HK and 3HAA to their corresponding nonphenolic analogues, kynurenine (KYN) and anthranilic acid (ANA), in aqueous solutions of Cu(II) at pH 7.41. Cyclic voltammetry of the four catabolite compounds in the absence of Cu(II) (data not shown) revealed no significant redox activity in the +0.15 to −0.4 V potential window compared to the PBS background (scan a in each panel). At potentials above +0.15 V, the catabolites undergo direct irreversible oxidation, a reaction that is not considered further here. Cyclic voltammetry of Cu(II) in PBS yielded a current response at ≈ −100 mV due to reduction of the metal ion (scan b in each panel). In the presence of either KYN or ANA, the Cu(II) reduction wave was largely unaffected (KYN and ANA panels, scan c) although KYN appears to show some slight reactivity. This result suggests that most of the Cu(II) remains uncomplexed and available for reduction in the presence of these two catabolites. The Cu(II) reduction wave was nearly abolished in the presence of 3HK (3HK panel, scan c), and markedly decreased in the presence of 3HAA (3HAA panel, scan c). These results indicate that loss of electrochemically active Cu(II) by complexation and/or reduction occurs readily in the presence of 3HK and 3HAA, but not in the presence of KYN or ANA. These findings are consistent with the proposed reduction of Cu(II) by 3HK and 3HAA.

We next examined whether superoxide is generated by the reaction of 3HK and 3HAA with Cu(II) (Figure 4). We found significant superoxide production by 3HK and 3HAA

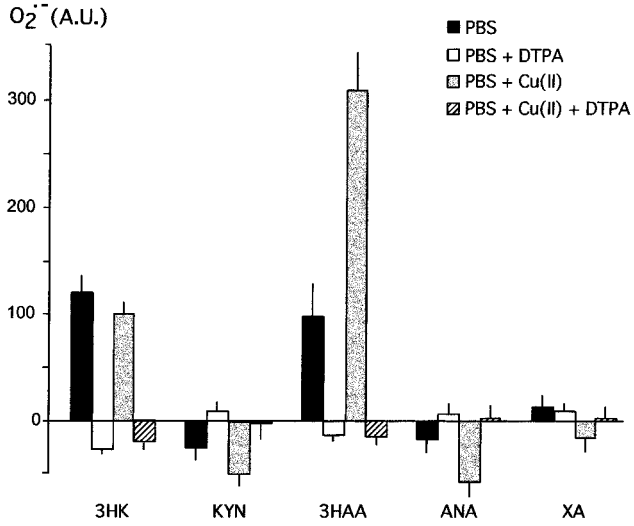

FIGURE 4: Superoxide production by kynurenine catabolites. Generation of superoxide by kynurenine catabolites (10 μM) in the dark for 1 h at 37 °C. Reactions were conducted either in the absence of added Cu(II) (CON) or in the presence of added Cu(II) (1 μM). Values represent the mean ± SD for three independent measurements.

in agreement with others [e.g., see (*50*)]. In the present study, we demonstrated that superoxide production occurs under both trace metal and copper-supplemented conditions for 3HK and 3HAA, but not KYN, ANA, or XA. Superoxide generation by 3HAA, but not 3HK, was promoted by the

addition of Cu(II). We noted that this Cu(II) potentiation superoxide generation by 3HAA was linearly increased by increasing concentration of the metal (data not shown). Addition of the chelator DTPA potently inhibited superoxide production by 3HK and 3HAA, indicating that superoxide generation by 3HK and 3HAA are metal-dependent reactions.

Since both 3HK and 3HAA reduced Cu(II) and generated superoxide, we next studied the possible formation of hydrogen peroxide. Based on our recent observations on the Alzheimer Disease $A\beta_{(1-42)}$ peptide−Cu complex (*46*), we examined hydrogen peroxide production by 3HK in the presence of Cu(II) under conditions of high, ambient, and low oxygen tension (Figure 5A). Reactions were conducted in the dark to avoid photodynamic effects. Only small amounts of hydrogen peroxide were produced by Cu(II) alone under all three oxygen tension conditions (high O_2: 0.10 μM H_2O_2; ambient O_2: 0.11 μM H_2O_2; low O_2: 0.09 μM H_2O_2). When 3HK was added to the incubation solution, hydrogen peroxide production was markedly increased under the high and ambient oxygen tension conditions (1.84 μM H_2O_2 and 1.49 μM H_2O_2, respectively). However, when the oxygen tension of the incubation solution was lowered by continuous argon sparging, production of hydrogen peroxide was markedly inhibited (0.35 μM H_2O_2), indicating that molecular oxygen dissolved in the reaction buffer is a substrate for hydrogen peroxide production. Next, we investigated the time dependence of hydrogen peroxide generation at 37 °C in the dark. The generation of hydrogen peroxide by both 3HK and ascorbate, the positive control, was continuous over 5 h (Figure 5B), indicating that neither 3HK nor ascorbate is consumed over the time course of the present experiments. Copper may act catalytically in this situation, cycling between the reduced state (fostered by reaction with 3HK) and the oxidized state (promoted by reaction with molecular oxygen).

We next compared the metal dependence of 3HK and 3HAA compared to KYN or ANA in their ability to generate hydrogen peroxide (Figure 5C). Under control conditions using Chelex resin-treated PBS to remove trace metal ions, no hydrogen peroxide was generated. Only a small quantity (approximately 0.3 μM) of hydrogen peroxide was generated when Cu(II) alone (1 μM) or the nonphenolic catabolites KYN or ANA were added to the Chelex resin-treated PBS. However, addition of 3HK or 3HAA resulted in marked hydrogen peroxide generation (approximately 3 μM), which was abolished by addition of the hydrogen peroxide scavenging enzyme catalase. Hydrogen peroxide production by 3HK or 3HAA coincubated with Cu(II) was also abolished by addition of the copper chelator TETA, demonstrating the metal dependence of this reaction.

Although two Fenton chemistry substrates, hydrogen peroxide and reduced redox-active metal, are produced by 3HK and 3HAA, we did not detect evidence of the hydroxyl radical using the thiobarbituric acid-reactive substance assay (*46*) (data not shown). This result does not exclude hydroxyl radical production by the reaction of 3HK or 3HAA with Cu(II) since it is possible that the radical may be consumed at the site of generation before it has time to react with the TBARS indicator compound (discussed below).

We investigated the interaction of 3HK and 3HAA with total calf lens proteins in the presence or absence of Cu(II) (Figure 6). In these experiments, we monitored the lens

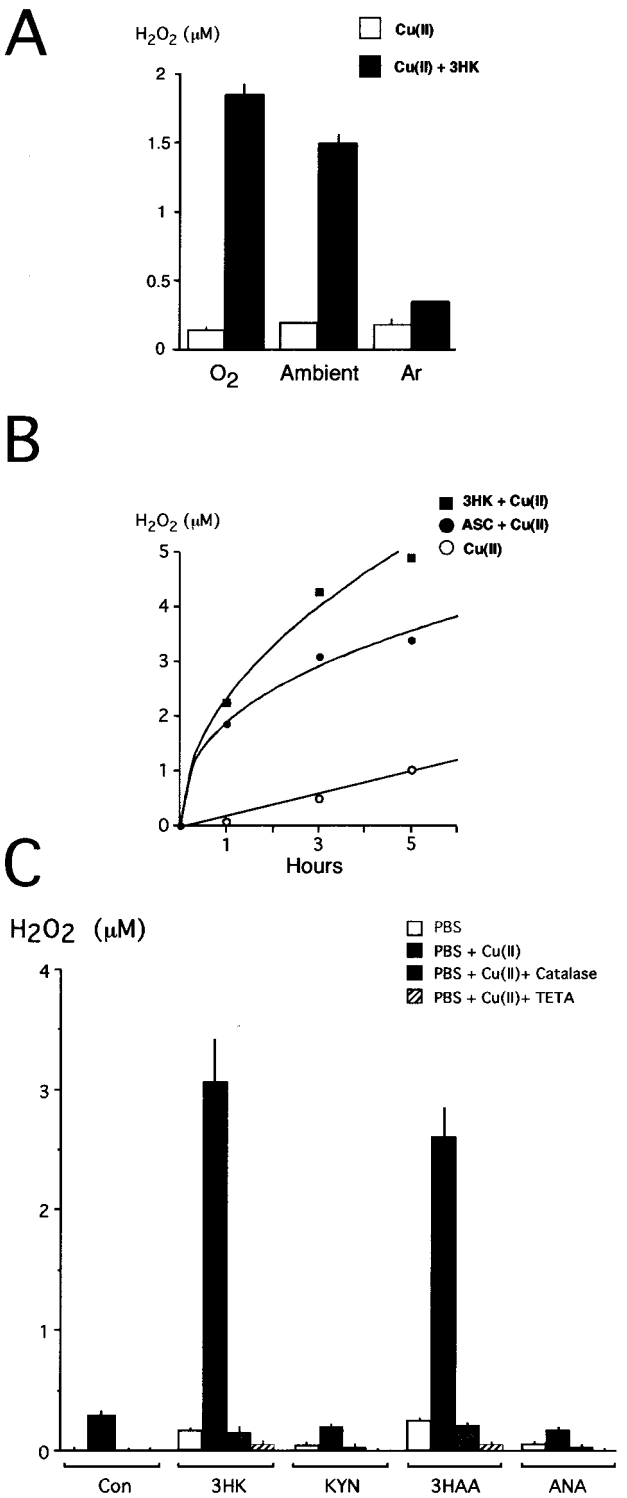

FIGURE 5: Production of hydrogen peroxide by kynurenine metabolites. Panel A: Concentration of hydrogen peroxide generated by Cu(II) (1 μM) ± 3HK (10 μM) in the presence of high (O_2), ambient (Ambient), or low oxygen tension (Ar: argon-sparged) after incubation at 37 °C for 1 h in the dark. Panel B: Time dependence of hydrogen peroxide formation by 3HK and ascorbate (ASC) in the dark. Hydrogen peroxide concentration generated by 3HK (10 μM) + Cu(II) (1 μM), ascorbate (ASC, 10 μM) + Cu(II) (1 μM), or Cu(II) (1 μM) alone. Values represent the mean ± SD, $n = 3$. Panel C: Generation of hydrogen peroxide by kynurenine catabolites (10 μM) under ambient gas conditions for 1 h at 37 °C in the dark. Reactions were conducted either in the presence or absence of added Cu(II) (1 μM) or in the presence of catalase (1000 units/mL) or the copper chelator TETA (200 μM), as indicated. Con = No added kynurenine catabolite. Values represent the mean ± SD for three independent measurements.

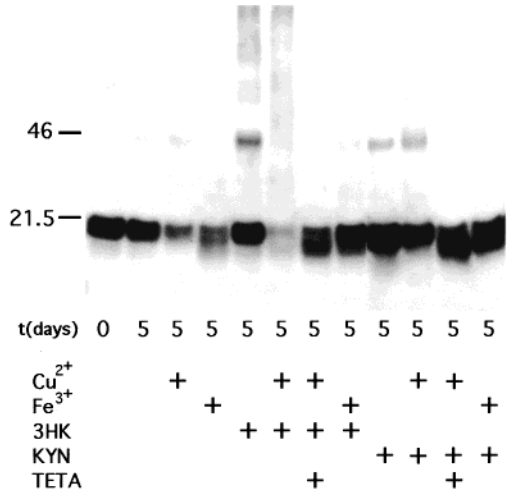

FIGURE 6: Promotion by kynurenine catabolites of SDS- and β-mercaptoethanol-resistant apparent cross-linked oligomers of α_B-crystallin. Western blot analysis of calf total lens protein (100 μg/mL) probed for α_B-crystallin. Protein samples were incubated for 5 days at 37 °C in the dark with Cu(II) (10 μM) or Fe(III) (10 μM), 3HK (10 μM) or KYN (10 μM), the copper chelator TETA (200 μM), or combinations as indicated. Incubation time (in days) is shown. A control sample of total lens protein was prepared and immediately frozen until assay and is shown in the first lane. Molecular weight markers are shown on the left.

structural protein α_B-crystallin migration by Western blot analysis. The incubations were conducted in the dark to avoid photodynamic effects. When 3HK was added to the incubation mixture, formation of SDS- and β-mercaptoethanol-resistant apparent dimers and higher order oligomers was observed. The 3HK-induced α_B-crystallin cross-linking effect was dramatically enhanced in the presence of Cu(II) (10 μM) and was abolished by coincubation with the copper chelator TETA. The apparent α_B-crystallin cross-linking promoted by coincubation of 3HK with Cu(II) was also accompanied by loss of the monomeric protein species and generation of smaller protein fragments (less than approximately 20 kDa). Addition of the copper chelator TETA reversed the depletion of monomeric α_B-crystallin when this protein was coincubated with 3HK and Cu(II). The presence of some apparent cross-linking observed with 3HK in the absence of added Cu(II) may be due to interaction with trace Cu(II) present in the incubation solution, since our buffer solutions, even after careful treatment with Chelex-100 resin, still contain approximately 0.1 μM total Cu background contamination as measured by inductively coupled plasma mass spectroscopy (data not shown). The Western blot results also indicated that incubation with the nonphenolic 3HK analogue, KYN, does induce α_B-crystallin cross-linking, but to a much reduced extent, consistent with the assays for metal reduction, superoxide generation, and hydrogen peroxide production. Cross-linking of α_B-crystallin did not occur when Fe(III) was substituted for Cu(II). Similar results were obtained when the Western blots were probed for α_A-crystallin (data not shown).

To exclude the effects of other lens proteins on the observed findings in Figure 6, we examined these interactions with purified recombinant human α_B-crystallin. After 5 days of incubation at 37 °C in the dark, α_B-crystallin was predominantly present as a monomer, even when coincubated with Cu(II) (Figure 7A). However, after incubation with

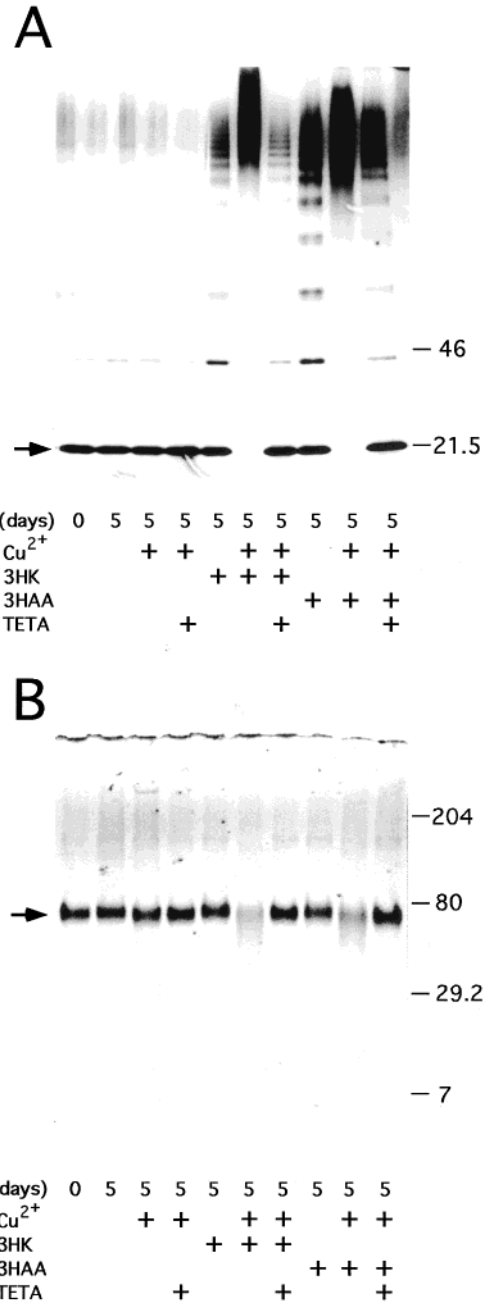

FIGURE 7: Promotion by kynurenine catabolites of SDS- and β-mercaptoethanol-resistant cross-linking of purified recombinant human α_B-crystallin. Silver staining for total protein after SDS−polyacrylamide gel electrophoresis of purified recombinant human α_B-crystallin (25 μg/mL; panel A) or bovine serum albumin (25 μg/mL; panel B) after incubation for 5 days, 37 °C, in the dark. Protein samples were incubated in the presence of Cu(II) (10 μM), 3HK (10 μM), 3HAA (10 μM), the copper chelator TETA (200 μM), or combinations as indicated. Incubation time (in days) is shown. A control sample of each protein was prepared and immediately frozen until assay and is shown in the first lane. Molecular weight markers are shown on the right. Arrowheads mark monomeric species.

3HK, apparent dimeric and higher order oligomers were observed (Figure 7A). After coincubation with Cu(II) and 3HK together, the monomeric and apparent dimeric α_B-crystallin species were not observed, and a prominent high molecular weight smear became apparent. This effect was substantially attenuated by the copper chelator TETA. Addition of TETA substantially reversed the apparent cross-linking of monomeric α_B-crystallin when incubated with

3HK and Cu(II). Interactions with 3HAA produced a similar pattern of Cu(II)-dependent apparent oligomerization and loss of the monomer which was reversed with TETA. Mass spectroscopy analysis of the products observed by electrophoresis and silver staining confirmed the presence of covalently cross-linked oligomers which matched the Western blot (data not shown). Incubation of recombinant α_B-crystallin with varying concentrations of Cu(II) alone up to concentrations of 20 μM did not result in observable apparent cross-linking or degradation (data not shown).

We compared the interaction of 3HK and 3HAA with Cu(II) in the presence of another target protein, bovine serum albumin (BSA; Figure 7B). After 5 days of incubation at 37 °C in the dark, BSA was predominantly present as a monomer, even when coincubated with Cu(II) (Figure 7B). In contrast to the findings with α-crystallin, we did not observe apparent dimeric and higher order oligomers after incubation with 3HK alone. After coincubation of 3HK with Cu(II), the monomer was no longer detectable without emergence of apparent cross-linked species. A faint smear was detectable between approximately 30 and 60 kDa. These results indicating loss of mass are consistent with fragmentation and degradation of the BSA monomer. Note that this apparent protein depletion effect was abolished by the copper chelator TETA. Interactions with 3HAA produced a similar pattern of apparent Cu(II)-dependent protein depletion. A similar pattern of protein depletion was observed when myelin basic protein was used as a target protein (data not shown). Thus, the oxidative cross-linking induced by 3HK and 3HAA in the presence of Cu(II) was specific for α-crystallin when compared to bovine serum albumin and myelin basic protein under the present experimental conditions.

Since the Fenton chemistry substrates hydrogen peroxide and reduced redox-active metal are generated by 3HK and 3HAA, we hypothesized that the cross-linking of α_B-crystallin might be mediated by generation of the hydroxyl radical. However, incubation of α_B-crystallin with either 3HK or 3HAA and Cu(II) in the presence of hydroxyl radical scavenging agents such as DMSO, mannitol, or salicylate did not inhibit the cross-linking of α_B-crystallin (data not shown). Similarly, neither catalase nor superoxide dismutase was capable of inhibiting the cross-linking of α_B-crystallin by 3HK or 3HAA in the presence of Cu(II) (data not shown).

We next examined whether treating calf lens α-crystallin with either 3HK or 3HAA would confer enhanced redox reactivity to α-crystallin by binding to the lysine residues of the protein (*20*). In these preparations, α-crystallin was incubated with the various kynurenine catabolites. Free catabolite was then removed by dialysis, and the resulting modified α-crystallin was tested for metal reduction capacity. Unmodified α-crystallin reduced approximately 35% of the available Cu(II) and a negligible amount of Fe(III) (Figure 8). In contrast, 3HK-modified α-crystallin reduced 100% of the available Cu(II) and approximately 20% of the available Fe(III). 3HAA-modified α-crystallin reduced approximately 65% of the available Cu(II). As a control incubation, we tested α-crystallin treated with ascorbate, another potent metal reducing agent. Ascorbate-modifed α-crystallin did not result in an increase in α-crystallin reducing activity when compared to unmodified α-crystallin, suggesting that the *o*-aminophenol kynurenine catabolites 3HK and 3HAA modify α-crystallin by binding to the protein and remaining redox-reactive. Studies are currently underway to address this hypothesis.

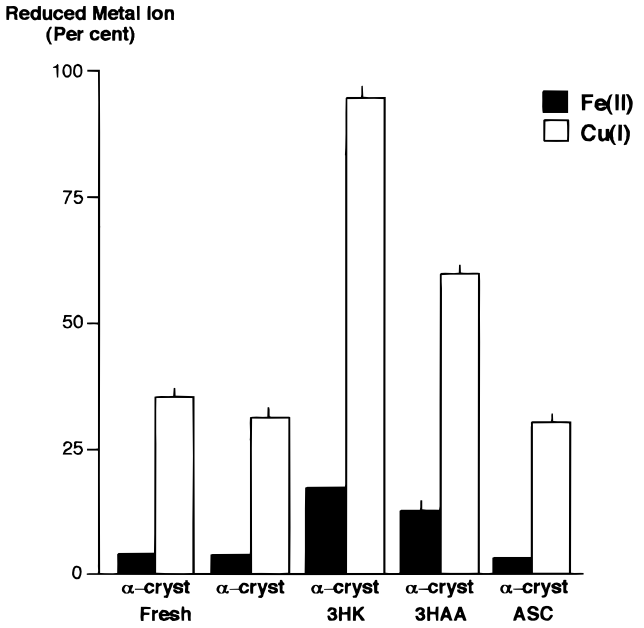

FIGURE 8: Electrochemical reduction of Cu(II) and Fe(III) by α-crystallin modified by 3HK and 3HAA. α-Crystallin modified by 3HK, 3HAA, or ASC was tested for metal reduction capacity. Free 3HK, 3HAA, or ASC was removed by exhaustive dialysis of the modified α-crystallin preparations. Fresh α-crystallin and unmodified α-crystallin treated in the absence of added catabolite were used as negative controls. Samples of each α-crystallin preparation (100 μg/mL) were coincubated with either Cu(II)-glycine (25 μM) or Fe(III)-citrate (25 μM) for 1 h at 37 °C and analyzed for metal reduction using the reduced metal indicators BC for Cu(I) and BP for Fe(II). Values represent the mean ± SD for three independent measurements.

DISCUSSION

These data demonstrated that the *o*-aminophenol kynurenine pathway catabolites, 3HK and 3HAA, but not their respective nonphenolic precursors, potently reduce Cu(II), and to a lesser extent Fe(III). In addition, both superoxide and hydrogen peroxide were generated by these compounds in a Cu-dependent manner. Hydrogen peroxide generation was also shown to require the presence of molecular oxygen. Taken together, these data indicate that 3HK and 3HAA both react with Cu(II) and molecular O_2 to produce H_2O_2.

The finding that neither L-kynurenine (the nonphenolic precursor of 3HK) nor anthranilic acid (the nonphenolic analogue of 3HAA) was capable of reducing the metal ions or generating superoxide and hydrogen peroxide highlights the importance of the phenolic hydroxyl group in mediating the observed reactions. Since both 3HK and 3HAA generated approximately 3-fold more hydrogen peroxide than available Cu(II), the copper is likely cycling between oxidized and reduced states, permitting multiple electron transfers. In the presence of total lens protein or purified recombinant α_B-crystallin, both 3HK and 3HAA promoted SDS- and β-mercaptoethanol-resistant apparent cross-linking of α_B-crystallin in a Cu-dependent manner. Both 3HK and 3HAA are also known to bind to lens proteins and α-crystallins directly through lysyl residues, resulting in aggregation, pigmentation, and development of a distinct blue (non-tryptophan) fluorescence (*15, 18, 20, 51*)—all properties characteristic of

nuclear cataract formation. We have also shown that α-crystallin, modified with either 3HK or 3HAA, has increased ability to reduce redox-active metal, especially Cu(II).

Most redox-active metals in biological systems are bound to protein and small biomolecules and are not present as free metal ions. However, two scenarios may be operative in the lens which argue for redox-active metal ion availability. First, protein-bound metal ions can be liberated by acidosis, a condition present in the nucleus of the lens (*52*). Thus, metal ions which may be less tightly bound to lenticular proteins may be more available for reaction with 3HK and 3HAA. This may also be the case of the glycated lens proteins in diabetes mellitus, resulting in elevated levels of less tightly bound metal ions (*45*). Second, the proposed reactions may be carried out in the local environment of the protein-bound metal. Therefore, an increase in free redox-active metal ions in the lens may not be obligatory for these reactions to occur. Indeed, protein-bound copper complexes can catalyze some reactions similar to those observed with free copper (*53, 54*). These mechanisms may not be mutually exclusive. The present data are consistent with a common redox biochemistry which may contribute to the oxidative damage noted in ARC. Furthermore, the present results suggest that targeted chelation of redox-active metal ions, or displacement with non-redox-active metals such as zinc, may have therapeutic potential in preventing or treating ARC.

We have found that only tryptophan metabolites possessing an *o*-aminophenol group (i.e., 3HK and 3HAA) are redox-active. The mechanism for the *o*-aminophenol effects is likely to involve equilibrium formation of anilino or phenoxyl radicals with subsequent decay through oxidation to a quinonimine structure (*22*) by disproportionation, or through dimerization and/or condensation. The observed increased redox activity of the *o*-aminophenol catabolites 3HK and 3HAA compared to their corresponding nonphenolic precursors may be due to resonance stabilization of the *o*-aminophenol-derived radicals. Alternatively, in the proteinaceous environment of the lens, the radicalized *o*-aminophenol catabolites could react with local proteins (e.g., such as α-crystallin), leading to protein radicalization, adduct formation, cross-linking, and fragmentation.

Our findings indicate that in the presence of substoichiometric amounts of Cu(II), 3HK and 3HAA simultaneously generate reduced redox-active metal ions and hydrogen peroxide, products that when combined could result in formation of the highly reactive hydroxyl radical by Fenton-type chemistry. We were unable to detect evidence of the hydroxyl radical in the thiobarbituric acid-reactive substance (TBARS) assay, and were similarly unable to suppress 3HK- and 3HAA-induced α_B-crystallin cross-linking with hydroxyl radical scavengers such as dimethyl sulfoxide, salicylate, or mannitol. Nor were we able to suppress α_B-crystallin cross-linking by decreasing hydrogen peroxide levels with catalase. These findings do not support a role for the hydroxyl radical in the aggregation of α_B-crystallin. However, we cannot conclusively exclude the possibility of hydroxyl radical generation since this highly reactive species may elude detection using our indirect assay methods. For example, 3HK and 3HAA may promote hydroxyl radical formation by Fenton chemistry and simultaneously serve as a site for hydroxyl radical attack (i.e., acts as a hydroxyl radical scavenger), consistent with other reports that 3HK has antioxidant properties (*55*−*57*). Indeed, other investigators have observed generation of the hydroxyl radical in ESR spin-trapping studies of 3HK and 3HAA in the presence of $FeCl_3$ and superoxide dismutase (*58*). A similar mechanism invoking hydroxyl radical generation has been postulated for 3HK- and 3HAA-induced damage to DNA, chromatid breakage and translocation (*59*). The reactivity of these vicinal aminohydroxy compounds with redox-active transition metal ions may be analogous to the redox cycling chemistry observed in vicinal dihydroxy compounds such as dopamine and related catecholamines (*60, 61*).

UV light-induced crystallin cross-linking is enhanced by 3HK and 3HAA (*62*). Our data, however, indicate that 3HK and 3HAA foster protein cross-linking even in the dark when Cu(II) is present. Indeed, the presence of redox-active metal ions appears to promote the cross-linking reaction since the addition of a chelator suppresses this reaction. In contrast to the effects of 3HK and 3HAA on the cross-linking of α_B-crystallin, these kynurenine catabolites fostered the degradation of bovine serum albumin and myelin basic protein (*63, 64*). The differences in 3HK- and 3HAA-induced protein oxidation may reflect the local protein microenvironment in which the *o*-aminophenol catabolites and Cu(II) react. Investigations are currently underway to address this issue.

The interaction of these kynurenine catabolites with redox-active metal ions and proteins may occur in a variety of biochemical settings. During conditions of local acidosis such as inflammation or infection, copper and iron are liberated from proteins and thus are made available for redox reactions and protein interactions (*65*−*67*). These conditions also activate cells of the macrophage/monocyte lineage. Indoleamine-2,3-dioxygenase, the rate-limiting enzyme in the kynurenine metabolic pathway, is induced by interferon-γ (*11, 12*), a factor released during inflammation and infection. Indoleamine-2,3-dioxygenase requires consumption of the superoxide anion generated during the macrophage respiratory burst for activity (Figure 1). The net result of these reactions is increased production of the kynurenine pathway catabolites, including 3HK and 3HAA, and presumably increased generation of reactive oxygen species such as superoxide and hydrogen peroxide.

The present data indicate that copper and iron are reduced by 3HK and 3HAA, even in the dark, fostering further generation of reactive oxygen species, resulting in subsequent protein damage. These actions may serve a physiological function during infection by damaging proteins of infectious agents and facilitating their functional inactivation, degradation, and clearance. However, inappropriate activation of this pathway may contribute to degenerative or inflammatory conditions by facilitating oxidative damage to important host proteins.

REFERENCES

1. Fukui, S., Schwarcz, R., Rapoport, S. I., Takada, Y., and Smith, Q. R. (1991) *J. Neurochem. 56*, 2007−2017.
2. Reynolds, G. P., and Pearson, S. J. (1989) *Lancet 2*, 979−980.
3. Pearson, S. J., and Reynolds, G. P. (1992) *Neurosci. Lett. 144*, 199−201.
4. Ogawa, T., Matson, W. R., Beal, M. F., Myers, R. H., Bird, E. D., Milbury, P., and Saso, S. (1992) *Neurology 42*, 1702−1706.

5. Sardar, A. M., Bell, J. E., and Reynolds, G. P. (1995) *J. Neurochem. 64*, 932−935.
6. Sanni, L. A., Thomas, S. R., Tattam, B. N., Moore, D. E., Chaudhri, G., Stocker, R., and Hunt, N. H. (1998) *Am. J. Pathol. 152*, 611−619.
7. Heyes, M. P., Saito, K., Major, E. O., Milstien, S., Markey, S. P., and Vickers, J. H. (1993) *Brain 116*, 1425−1450.
8. Heyes, M. P., Saito, K., Jacobowitz, D., Markey, S. P., Takikawa, O., and Vickers, J. H. (1992) *FASEB J. 6*, 2977−2989.
9. Munn, D. H., Zhou, M., Attwood, J. T., Bondarev, I., Conway, S. J., Marshall, B., Brown, C., and Mellor, A. L. (1998) *Science 281*, 1191−1193.
10. Flanagan, E. M., Erickson, J. B., Viveros, O. H., Chang, S. Y., and Reinhard, J. F., Jr. (1995) *J. Neurochem. 64*, 1192−1196.
11. Yoshida, R., Urade, Y., Tokuda, M., and Hayaishi, O. (1979) *Proc. Natl. Acad. Sci. U.S.A. 76*, 4084−4086.
12. Okuda, S., Nishiyama, N., Saito, H., and Katsuki, H. (1996) *Proc. Natl. Acad. Sci. U.S.A. 93*, 12553−12558.
13. Okuda, S., Nishiyama, N., Saito, H., and Katsuki, H. (1998) *J. Neurochem. 70*, 299−307.
14. Van Heyningen, R. (1971) *Nature 230*, 393−394.
15. Van Heyningen, R. (1973) *Exp. Eye Res. 15*, 121−126.
16. Hood, B. D., Garner, B., and Truscott, R. J. W. (1999) *J. Biol. Chem. 274*, 32547−32550.
17. Chiarugi, A., Rapizzi, E., and Moroni, F. (1999) *FEBS Lett. 453*, 197−200.
18. Wood, A. M., and Truscott, R. J. (1993) *Exp. Eye Res. 56*, 317−325.
19. Bando, M., Nakajima, A., and Satoh, K. (1981) *J. Biochem. (Tokyo) 89*, 103−109.
20. Stutchbury, G. M., and Truscott, R. J. (1993) *Exp. Eye Res. 57*, 149−155.
21. Wood, A. M., and Truscott, R. J. (1994) *Vision Res. 34*, 1369−1374.
22. Aquilina, J. A., Carver, J. A., and Truscott, R. J. (1999) *Biochemistry 38*, 11455−11464.
23. Chen, Y. C., Reid, G. E., Simpson, R. J., and Truscott, R. J. (1997) *Exp. Eye Res. 65*, 835−840.
24. Harding, J. J. (1972) *Biochem. J. 129*, 97−100.
25. Harding, J. J. (1998) *Curr. Opin. Ophthalmol. 9*, 10−13.
26. Dilley, K. J., and Pirie, A. (1974) *Exp. Eye Res. 19*, 59−72.
27. Augusteyn, R. C., and Koretz, J. F. (1987) *FEBS Lett. 222*, 1−5.
28. Horwitz, J. (1992) *Proc. Natl. Acad. Sci. U.S.A. 89*, 10449−10453.
29. Carver, J. A., Aquilina, J. A., Cooper, P. G., Williams, G. A., and Truscott, R. J. (1994) *Biochim. Biophys. Acta 1204*, 195−206.
30. Bhat, S. P., Horwitz, J., Srinivasan, A., and Ding, L. (1991) *Eur. J. Biochem. 202*, 775−781.
31. Groenen, P. J., Merck, K. B., de Jong, W. W., and Bloemendal, H. (1994) *Eur. J. Biochem. 225*, 1−19.
32. Rogers, K. M., and Augusteyn, R. C. (1978) *Exp. Eye Res. 27*, 719−721.
33. Fecondo, J. V., and Augusteyn, R. C. (1983) *Exp. Eye Res. 36*, 15−23.
34. Bhuyan, K. C., Bhuyan, D. K., and Podos, S. M. (1986) *Life Sci. 38*, 1463−1471.
35. Micelli-Ferrari, T., Vendemiale, G., Grattagliano, I., Boscia, F., Arnese, L., Altomare, E., and Cardia, L. (1996) *Br. J. Ophthalmol. 80*, 840−843.
36. Spector, A. (1984) *Ciba Found. Symp. 106*, 48−64.
37. Ramachandran, S., Morris, S. M., Devamanoharan, P., Henein, M., and Varma, S. D. (1991) *Exp. Eye Res. 53*, 503−506.
38. Cekic, O. (1998) *Br. J. Ophthalmol. 82*, 186−188.
39. Balaji, M., Sasikala, K., and Ravindran, T. (1992) *Br. J. Ophthalmol. 76*, 668−669.
40. Rasi, V., Costantini, S., Moramarco, A., Giordano, R., Giustolisi, R., and Balacco Gabrieli, C. (1992) *Ann. Ophthalmol. 24*, 459−464.
41. Srivastava, V. K., Varshney, N., and Pandey, D. C. (1992) *Acta Ophthalmol. (Copenhagen) 70*, 839−841.
42. Racz, P., and Erdohelyi, A. (1988) *Ophthalmic Res. 20*, 10−13.
43. Cook, C. S., and McGahan, M. C. (1986) *Curr. Eye Res. 5*, 69−76.
44. Nath, R., Srivastava, S. K., and Singh, K. (1969) *Ind. J. Exp. Biol. 7*, 25−26.
45. Lin, J. (1997) *Jpn. J. Ophthalmol. 41*, 130−137.
46. Huang, X., Atwood, C. S., Hartshorn, M. A., Multhaup, G., Goldstein, L. E., Scarpa, R. C., Cuajungco, M. P., Gray, D. N., Lim, J., Moir, R. D., Tanzi, R. E., and Bush, A. I. (1999) *Biochemistry 38*, 7609−7616.
47. Sun, T. X., Das, B. K., and Liang, J. J. (1997) *J. Biol. Chem. 272*, 6220−6225.
48. Bindokas, V. P., Jordan, J., Lee, C. C., and Miller, R. J. (1996) *J. Neurosci. 16*, 1324−1336.
49. Sayre, L. M. (1996) *Science 274*, 1933−1934.
50. Linetsky, M., James, H. L., and Ortwerth, B. J. (1999) *Exp. Eye Res. 69*, 239−248.
51. Benavente, M. G., and Truscott, R. J. (1991) *Arch. Biochem. Biophys. 290*, 451−457.
52. Mathias, R. T., Riquelme, G., and Rae, J. L. (1991) *J. Gen. Physiol. 98*, 1085−1103.
53. Starkebaum, G., and Harlan, J. M. (1986) *J. Clin. Invest. 77*, 1370−1376.
54. Ehrenwald, E., Chisolm, G. M., and Fox, P. L. (1994) *J. Clin. Invest. 93*, 1493−1501.
55. Luthra, M., and Balasubramanian, D. (1992) *Exp. Eye Res. 55*, 641−643.
56. Christen, S., Peterhans, E., and Stocker, R. (1990) *Proc. Natl. Acad. Sci. U.S.A. 87*, 2506−2510.
57. Goshima, N., Wadano, A., and Miura, K. (1986) *Biochem. Biophys. Res. Commun. 139*, 666−672.
58. Kuznezova, L. E. (1969) *Nature 222*, 484−485.
59. Hiraku, Y., Inoue, S., Oikawa, S., Yamamoto, K., Tada, S., Nishino, K., and Kawanishi, S. (1995) *Carcinogenesis 16*, 349−356.
60. Bindoli, A., Rigobello, M. P., and Deeble, D. J. (1992) *Free. Radical Biol. Med. 13*, 391−405.
61. Levay, G., Ye, Q., and Bodell, W. J. (1997) *Exp. Neurol. 146*, 570−574.
62. Zigler, J. S., Jr., and Goosey, J. D. (1981) *Photochem. Photobiol. 33*, 869−874.
63. Dykens, J. A., Sullivan, S. G., and Stern, A. (1987) *Biochem. Pharmacol. 36*, 211−217.
64. Truscott, R. J., and Martin, F. (1989) *Exp. Eye Res. 49*, 927−940.
65. Halliwell, B., Gutteridge, J. M., and Blake, D. (1985) *Philos. Trans. R. Soc. London, Ser. B: Biol. Sci. 311*, 659−671.
66. Halliwell, B., and Gutteridge, J. M. (1984) *Biochem. J. 219*, 1−14.
67. Gutteridge, J. M. (1987) *Biochem. J. 245*, 415−421.

BI992997S